Research articles

Comparative study of the magnetic phase diagrams and spin-flop-driven magnetodielectric responses of the pure and Mn^{3+}-doped $Pb_2Fe_2Ge_2O_9$ single crystals

A. Pankrats [a,b,*], M. Kolkov [a], A. Balaev [a], A. Freidman [a,b], A. Vasiliev [a,b], D. Balaev [a,b]

[a] *Kirensky Institute of Physics, Krasnoyarsk Scientific Center, Siberian Branch, Russian Academy of Sciences, Krasnoyarsk 660036, Russia*
[b] *Siberian Federal University, Krasnoyarsk 660041, Russia*

A R T I C L E   I N F O

A B S T R A C T

The $Pb_2Fe_{2-x}Mn_xGe_2O_9$ (x = 0.43) orthorhombic antiferromagnet single crystals have been synthesized by a modified pseudo-flux technique and their magnetic and magnetodielectric properties have been investigated. It has been established that partial substitution of highly anisotropic Mn^{3+} ions for iron ones significantly affects the magnetic structure of the crystal. Under magnetization of the crystal along the rhombic *b* and *c* axes, magnetization jumps have been detected, which are indicative of the occurrence of orientational transitions identified as first-order ones. No weak ferromagnetism characteristic of the pure crystal in the rhombic *a* axis direction has been detected. The field dependences of the magnetization for the pure and Mn-doped crystals have been analyzed using the thermodynamic potential that takes into account the crystal symmetry. It has been shown that, in the Mn-substituted crystal, the antiferromagnetic vector in the ground state is parallel to the rhombic *b* axis; in this state, weak ferromagnetism has not been observed. Under magnetization along the *b* axis, a conventional spin-flop transition occurs. The orientational transition under magnetization along the *c* axis has been attributed to the reorientation of the antiferromagnetic vector relative to the *a* axis with the simultaneous occurrence of a weak ferromagnetic moment along the *c* axis. Magnetic phase diagrams of the Mn-doped crystal for the magnetic fields **H**||*b* and **H**||*c* have been built.

In the Mn-doped crystal, at **E**||*c* and **H**||*c*, the orientational transition-induced magnetodielectric response jump has been detected, which is higher than the jumps observed for the undoped crystal by a factor of 3. The magnetodielectric properties of the pure and Mn-doped crystals have been analyzed using their magnetic phase diagrams.

1. Introduction

New promising multifunctional materials provide a basis for the development of advanced microelectronic devices. The search for such materials and study of their characteristics are top priorities of modern solid state physics. In the last two decades, much attention has been paid to the synthesis of multifunctional materials with the tightly interrelated magnetic and electrical properties.

The multiferroic properties of compounds are thought to be induced, in particular, by ions with intriguing stereochemical properties, along with 3d ions responsible for the magnetic properties. These can be Bi^{3+} and Pb^{2+} ions, in which 6 s^2 valence electrons are not involved in the formation of chemical bonds with neighboring ions, but form the so-

called lone electron pairs. The ions with unsaturated bonds are characterized by the high polarizability and can form local dipole moments. The resulting polarized state worsens the structural stability of a compound and can lead to the formation of a ferroelectric state [1,2]. In addition, the presence of dipoles leads to strong distortions of both the "own" polyhedra and the neighboring octahedra containing 3d ions and thereby directly affect the state of a magnetic subsystem in the crystals. In particular, in the $Pb_{1-x}Ba_xFe_{1/2}Nb_{1/2}O_3$ crystals with a perovskite structure, such distortions of the oxygen environment of a 3d ion evoke the dependence of the magnetic phase transition temperature on the lead content [3].

A few years ago, our attention has been drawn by a Pb-containing compound the crystalline iron germanate $Pb_2Fe_2Ge_2O_9$ [4]. The study

---

* Corresponding author.
  E-mail address: pank@iph.krasn.ru (A. Pankrats).

of the magnetic properties of this crystal [5,6] showed that it is an orthorhombic antiferromagnet with weak ferromagnetism. The investigations of the magnetodielectric properties disclosed their strong dependence on the magnetic structure of the crystal. In particular, jumps of the magnetodielectric response induced by the spin-flop transition were found.

An effective way of controlling the magnetic structure of a crystal is doping with ions of a different sort. In particular, mixed doping of the rare-earth subsystem, along with its diamagnetic dilution, is widely used to govern the magnetic structure and magnetoelectric properties of rare-earth ferroborates with a *huntite* structure [7–9]. In our recent works, we used doping to modify the magnetic structure of the $PbMnBO_4$ crystal, in which partial substitution of Fe^{3+} ions in the manganese subsystem led to the transformation of the initial $PbMnBO_4$ ferromagnetic structure [10] to the ferrimagnetic-like structure of the doped crystal [11].

The known minerals *melanotekite* $Pb_2Fe_2Si_2O_9$ and *kentrolite* $Pb_2Mn_2Si_2O_9$ [12] have similar orthorhombic structures and are silicate analogs of the $Pb_2Fe_2Ge_2O_9$ crystal. The recent study of the magnetic properties of polycrystalline kentrolite showed [13] that, at low temperatures, this compound exhibits antiferromagnetic properties. The similarity of the melanotekite and kentrolite crystal structures allows the formation of the $Pb_2(Mn, Fe)_2Si_2O_9$ solid solution, the structural properties of which were examined in [14]. This suggests the possibility of partial substitution of manganese ions for iron ones in the $Pb_2Fe_2Ge_2O_9$ iron germanate crystal. In this case, the replacement of weakly anisotropic Fe^{3+} S-ions by Mn^{3+} ions with the high magnetic anisotropy intrinsic of the Jahn–Teller $3d^4$ ions holds the promise of a significant impact of such doping on the magnetic structure of the doped crystal.

This work is devoted to a comparative study of the magnetic phase diagrams and magnetodielectric properties of the pure and Mn-doped $Pb_2Fe_2Ge_2O_9$ single crystals. In the Mn-substituted crystal, the first-order orientational phase transitions under magnetization along the rhombic b and c axes were established. The field dependences of the magnetization of the crystals were analyzed using the thermodynamic potential that takes into account the crystal symmetry. The magnetic phase diagrams of the Mn-doped crystal for two orientations of the magnetic field relative to the crystal axes were built. A jump in the magnetodielectric response induced by the orientational transition was found. The magnetodielectric properties of the pure and Mn-doped crystals were examined using their magnetic phase diagrams.

2. Experimental

The synthesis of pure $Pb_2Fe_2Ge_2O_9$ single crystals by a modified pseudo-flux spontaneous crystallization technique and characterization of the obtained samples were described in [5,6]. The $Pb_2Fe_{2-x}Mn_xGe_2O_9$ single crystals were grown using the same technique. As in the synthesis of pure $Pb_2Fe_2Ge_2O_9$, to prevent contamination with foreign impurities, we only used the conventional $PbO–Ge_2O_3$ solvents contained in the chemical formula of the synthesized compound. The ratio between the main components and the solvent was 1 : 2. The thoroughly mixed oxides were placed in a platinum crucible and heated to a temperature of 1050 °C. After exposure at this temperature for 4 h, the crucible was cooled to 720 °C at a rate of 3.2 °C/h. Then, the synthesized crystals up to $1.5 \times 1.5 \times 3$ mm^3 in size were mechanically withdrawn from the crucible.

The X-ray diffraction (XRD) analysis of the $Pb_2Fe_{2-x}Mn_xGe_2O_9$ sample on a SMART PHOTON II single-crystal X-ray diffractometer confirmed its single-crystal structure and revealed no twinning or foreign phase impurities. The partial substitution of manganese ions for iron ones led to a slight increase in the crystal lattice parameters: a = 7.1631(5) Å, b = 11.2161(8) Å, and c = 10.1654(8) Å (compare with the values a = 7.149(3) Å, b = 11.177(4) Å, and c = 10.144(3) Å for the pure $Pb_2Fe_2Ge_2O_9$ crystal [5]).

It should be noted, however, that the determined symmetry of the substituted crystal is ambiguous: the coexistence of two orthorhombic space groups *Pbcn* and $P2_122_1$ with very close lattices is possible. This is apparently due to the effect of the partial replacement of iron by manganese. A crystal analogue of the crystals under study is the family of silicates, in which *melanotekite* $Pb_2Fe_2Si_2O_9$ crystallizes in the sp. gr. *Pbcn*, and *centrolite* $Pb_2Mn_2Si_2O_9$, in the sp. gr. $P2_122_1$ [12]. In the literature, we failed to find references to studies on the $Pb_2Mn_2Ge_2O_9$ crystal structure, but it can be assumed that, if such a compound exists, then its structure is also described by the sp. gr. $P2_122_1$. Then, at first glance, the coexistence of two space groups in a crystal could be indicative of the coexistence of two macroscopic phases ($Pb_2Fe_2Ge_2O_9$ and $Pb_2Mn_2Ge_2O_9$) in it. However, this contradicts the data on the distribution of manganese impurities in the substituted crystals.

The true manganese content in the crystals was determined by the X-ray fluorescence analysis on a Hitachi TM-3000 scanning electron microscope. To exclude the effect of contaminations and defect states on the natural faces, the concentration analysis was performed on the fresh-cleaved single-crystal surface (Fig. 1a); the spot type was 5–10 μm. Fig. 1b presents energy dispersive spectroscopy (EDS) elemental mapping images of manganese on the fresh-cleaved crystal surface. The images show that manganese is uniformly distributed throughout the sample, at least in a scale of 200–300 nm. Consequently, in the substituted single crystal, the separate $Pb_2Fe_2Ge_2O_9$ and $Pb_2Mn_2Ge_2O_9$ macroscopic phases do not form.

Table 1 gives the normalized iron and manganese contents obtained from the points shown in Fig. 1b. The average manganese content was found to be x = 0.43, which is similar to that in the charge (x = 0.4). The deviation of the Mn content from the average value at different points of the single crystal was no more than ± 5%.

The crystal orientation was determined from the XRD pattern of reflections from the largest sample face obtained on a Bruker D8 ADVANCE X-ray diffractometer. Fig. 1c shows XRD patterns of the pure and doped single crystals. The indexed peaks correspond to the reflections from the (1 1 0) crystal planes for both samples. The rest peaks marked by asterisks belong to the cell in which the sample was placed. The lower panel in Fig. 1c shows the XRD spectrum of the cell, which forms a background in the XRD patterns for both single crystals. The data obtained showed no twinning and confirmed the high crystal quality of the samples.

Fig. 2a shows the Laue pattern of the $Pb_2Fe_{1.57}Mn_{0.43}Ge_2O_9$ single crystal obtained with the primary beam perpendicular the (1 1 0) plane on a Photonic Science Laue crystal orientation system. Double or ring reflections are not observed, which is indicative of the single-crystal nature of the crystal. The absence of foreign phases is pointed out by good agreement between the experimental X-ray Laue diffraction pattern and the theoretical pattern built for sp. gr. *Pbcn* and the $Pb_2Fe_{1.57}Mn_{0.43}Ge_2O_9$ lattice parameters (Fig. 2b).

The field and temperature dependences of the magnetization for the $Pb_2Fe_{2-x}Mn_xGe_2O_9$ crystal were measured on a vibrating sample magnetometer (VSM) with a superconducting solenoid in magnetic fields of up to 70 kOe [15] and on a Quantum Design Physical Property Measurement System PPMS-9.

To study the magnetodielectric effect, two parallel faces perpendicular to the c axis were prepared. The faces were coated by an EPOTEK H20E electrically conductive epoxy-based glue. The samples prepared in this manner represented capacitors, which made it possible to apply an electric field parallel to the c axis. An experimental setup for studying the magnetodielectric effect was placed into a VSM cryostat [15]. The electric capacitance was measured as a function of temperature and magnetic field with an Agilent E4980A LCR meter at a frequency of 100 kHz using a four-wire circuit.

3. Experimental results

Fig. 3 shows temperature dependences of the magnetization for the $Pb_2Fe_{1.57}Mn_{0.43}Ge_2O_9$ crystal measured using a VSM with a superconducting solenoid in a magnetic field of 1 kOe applied along the main
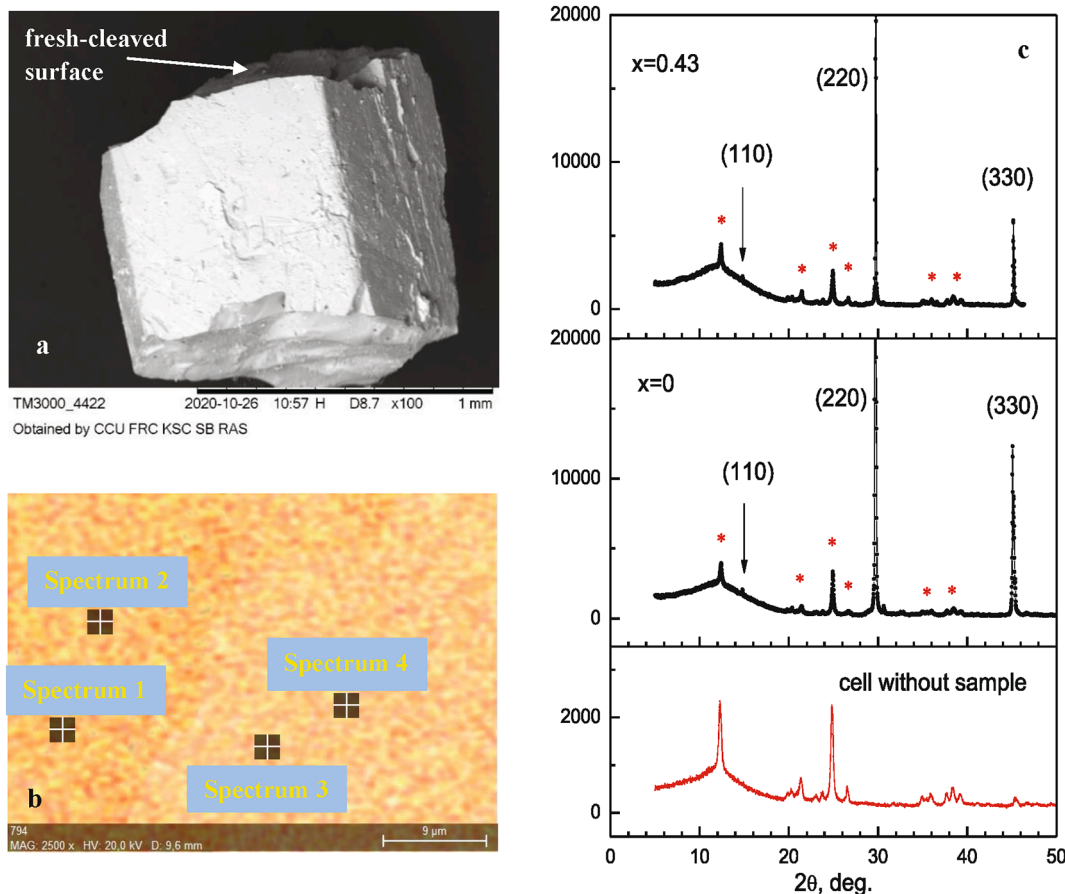
Fig. 1. (a) SEM image of the $Pb_2Fe_{1.57}Mn_{0.43}Ge_2O_9$ single crystal, (b) EDS elemental mapping image of manganese on the fresh-cleaved $Pb_2Fe_{1.57}Mn_{0.43}Ge_2O_9$ single crystal surface, and (c) XRD pattern of reflections from the (1 1 0) planes of the $Pb_2Fe_{2-x}Mn_xGe_2O_9$ single crystals with x = 0 and 0.43 and the cell XRD pattern (lower panel).

Table 1
The normalized concentration of iron and manganese of the $Pb_2Fe_{2-x}Mn_xGe_2O_9$ sample.

Spectrum #	Fe content (at %)	Mn content (at %)	x	<x>
Spectrum 1	78.1	21.9	0.44	0.43 ± 0.02
Spectrum 2	79.5	20.5	0.41	
Spectrum 3	78.5	21.5	0.43	
Spectrum 4	78.5	21.5	0.43	

orthorhombic directions. These dependences are qualitatively different from the dependences for pure $Pb_2Fe_2Ge_2O_9$ [5,6]. It concerns, first of all, the **H**||**a** direction (inset in Fig. 3). In the pure crystal, in this direction, below the Néel temperature T_N = 45.2 K, we observed the magnetization induced by the weak ferromagnetic moment, which monotonically increased with decreasing temperature, demonstrating the temperature dependence typical of the spontaneous magnetic moment. Upon doping of the crystal, the Néel temperature decreased and its value T_N = 39.9 K was determined from the maximum of the derivative dM/dT for the **a** axis. It can be seen in Fig. 3 that, in the Mn-doped crystal, just below T_N, the magnetization in this direction also first sharply increases, but below a temperature of T = 36 K, starts decreasing and, at low temperatures, drops to a value lower than the magnetization of pure $Pb_2Fe_2Ge_2O_9$ by an order of magnitude. In this case, the ZFC and FC dependences almost coincide, which is also different from the case of the pure crystal [5]. In addition, in pure $Pb_2Fe_2Ge_2O_9$, the magnetization in the rhombic **c** axis direction is minimum and its temperature dependence is typical of the easy magnetization axis. In the Mn-doped crystal, the minimum magnetization with the similar temperature

dependence was detected in the rhombic **b** axis direction.

Even more fundamental differences can be observed in the field dependences of the magnetization. In pure $Pb_2Fe_2Ge_2O_9$, the study of the field dependences disclosed weak ferromagnetism in the rhombic **a** axis direction and a spin-flop transition under magnetization along the **c** axis. Moreover, above the critical field of the spin-flop transition, we observed the field-induced weak ferromagnetic state with the moment M_{dc} almost twice as high as the spontaneous moment M_{da} in the **a** axis direction. Fig. 4 presents field dependences of the magnetization measured on the Mn-doped crystal at T = 4.2 K along the three rhombic axes. In this case, the spontaneous weak ferromagnetism in the **a** axis direction is not observed. The magnetization jumps indicative of the orientational transitions are observed in the directions of both the rhombic **b** and **c** axis. On the other hand, similar to the undoped $Pb_2Fe_2Ge_2O_9$ compound, under magnetization along the **c** axis in fields above the orientational transition, a weak ferromagnetic state is also established and has the same weak ferromagnetic moment ($M_{dc} \approx 1.8$ emu/g) as in the pure crystal.

The families of field dependences of the magnetization for the magnetic field orientations **H**||**b** and **H**||**c** were obtained on a Quantum Design Physical Property Measurement System PPMS-9 in magnetic fields of up to 70 kOe (Figs. 5 and 6) at different temperatures. Judging by the significant magnetic hysteresis in the region of orientational transitions, these transitions are first-order for both directions. In the field direction **H**||**b** (Figs. 4 and 5), we should note the following features. At low temperatures, the initial magnetic susceptibility below the critical field ($H < H_c$) is much weaker than the susceptibility above the orientational transition; upon approaching the Néel temperature, this susceptibility difference decreases. In addition, the measurements on a
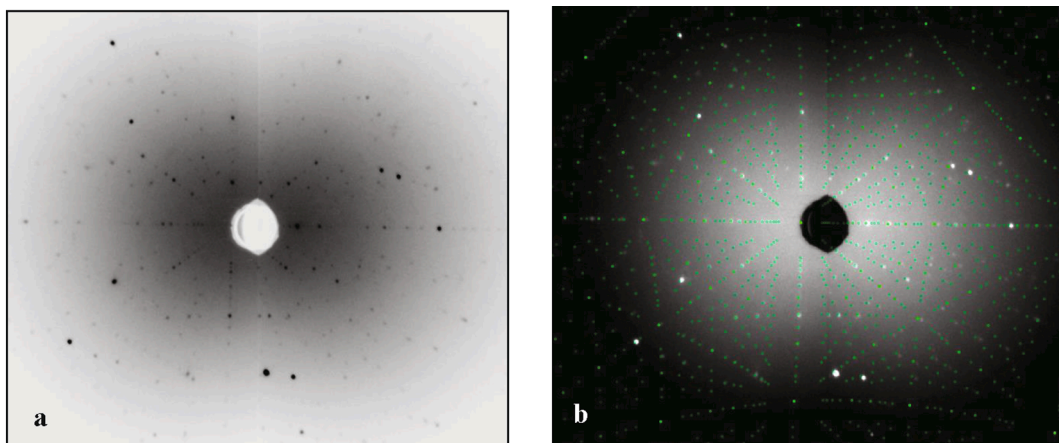
Fig. 2. (a) Experimental Laue X-ray diffraction pattern from the (1 1 0) crystallographic plane of the $Pb_2Fe_{1.57}Mn_{0.43}Ge_2O_9$ single crystal and (b) the same experimental pattern combined with the theoretical one.
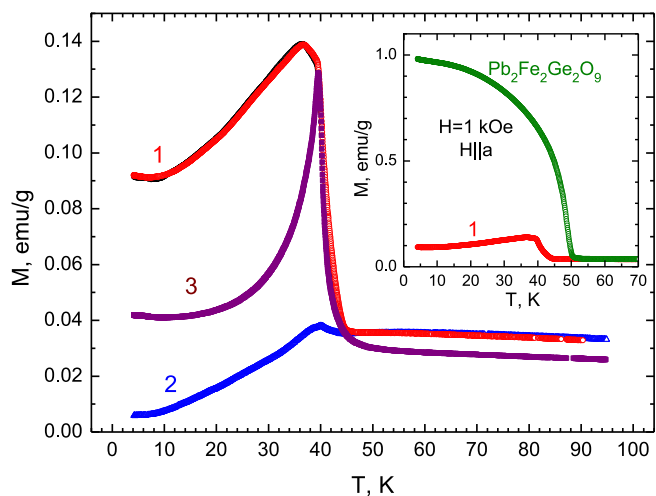

Fig. 3. Temperature dependences of magnetization for $Pb_2Fe_{1.57}Mn_{0.43}Ge_2O_9$ in a field of H = 1 kOe. The field directions are (1) $H||a$ ZFC (red) and FC (black), (2) $H||b$, and (3) $H||c$. Inset: magnetizations of the pure and Mn-doped crystals in the field $H||a$.
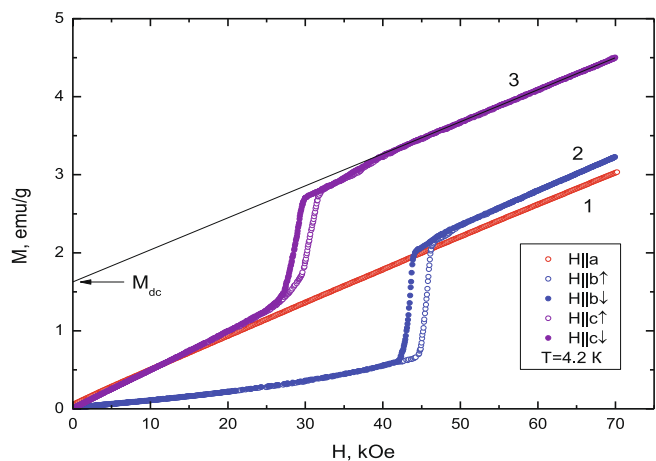

Fig. 5. Field dependences of magnetization for the $Pb_2Fe_{1.57}Mn_{0.43}Ge_2O_9$ crystal in the b axis direction measured at different temperatures.

Fig. 4. Field dependences of magnetization for the $Pb_2Fe_{1.57}Mn_{0.43}Ge_2O_9$ crystal measured at T = 4.2 K in the three orthorhombic directions.
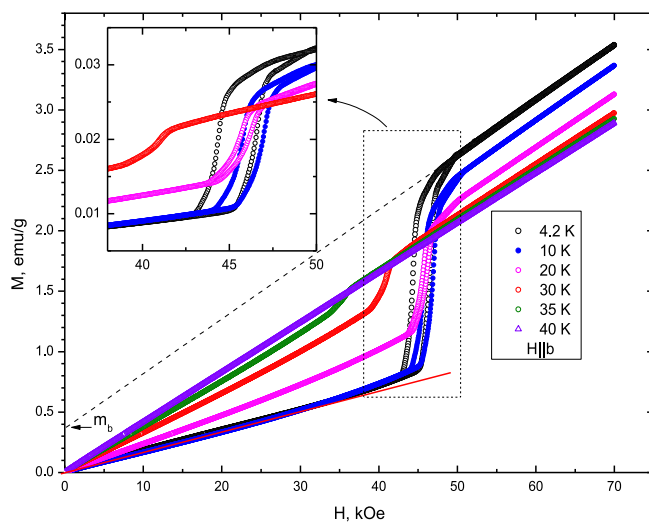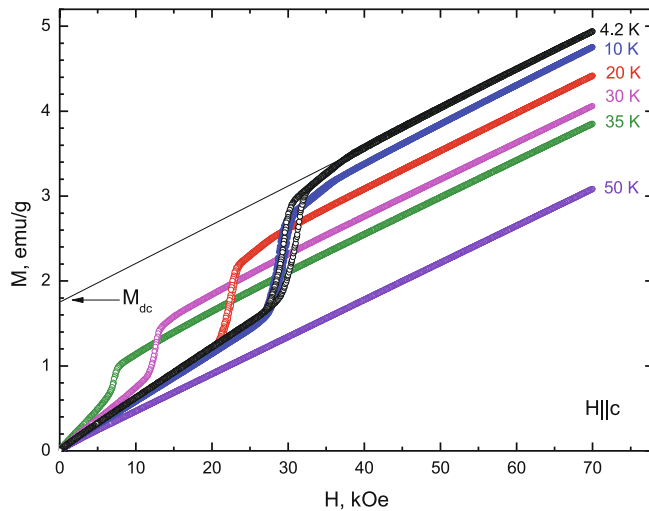

Fig. 6. Field dependences of magnetization for the $Pb_2Fe_{1.57}Mn_{0.43}Ge_2O_9$ crystal in the c axis direction measured at different temperatures.

PPMS-9 system in the state above the orientational transition at a temperature of 4.2 K revealed a weak ferromagnetic moment of $M_b \sim 0.35$ emu/g, which rapidly vanished with increasing temperature. It is noteworthy that the data in Fig. 4 obtained on the same crystal also show a low (~0.15 emu/g) weakly ferromagnetic moment at helium temperature. According to these data, for each new positioning of the sample, as well as for different samples, this moment ranges within 0.10 ÷ 0.35 emu/g. Such a great spread of the weak ferromagnetic moment suggests that this effect is "parasitic" and caused by inaccuracy of the sample orientation and admixing of the weak ferromagnetic moment arising in the field-induced state along the other crystal axis. The discussion of the origin of this induced moment is continued in Section 4.

Under magnetization along the rhombic c axis (Figs. 4 and 6), the magnetic susceptibilities before and after the transition are almost the same. As for the temperature dependences of the critical fields H_{SR}^b and H_{SR}^c, they are significantly different for the b and c directions. It can be seen in Fig. 5 (inset) that, as the temperature rises from liquid helium, the critical field for the b direction first slightly increases and, with a further increase in temperature, gradually decreases and then sharply drops upon approaching T_N. At the same time, the critical field for the c axis monotonically and almost linearly decreases with increasing temperature. Fig. 7 shows the temperature dependences of the critical fields, which were taken to be midpoints of the magnetization jumps with increasing field. In addition, the figure shows the temperature dependence of the field-induced weak ferromagnetic moment M_{dc} at $H||c$.

The angular dependence of the critical field in the rhombic bc plane was obtained in an attempt to measure the antiferromagnetic resonance (AFMR) in this crystal. This attempt was made using a magnetic resonance spectrometer with a pulsed magnetic field [16]. At frequencies of up to 110 GHz, no AFMR signal was detected; however, the reflected microwave signal contained singularities corresponding to the magnetic fields at which the orientational transitions occur. Fig. 8a shows fragments of the microwave reflection spectra measured at different frequencies in the magnetic field making an angle of $\varphi = 84°$ with the rhombic c axis. The positions of the field singularities are independent of the measuring frequency; therefore, it is reasonable to attribute these anomalies to the change in the microwave signal reflected from the short-circuited waveguide with the sample upon variation in its magnetic state. Thus, the observed anomalies are a nonresonance microwave response corresponding to the spin reorientation in the crystal. Such nonresonance microwave responses were observed by us, in particular, at the spin reorientation in the PbMnBO₄ crystal with partial substitution of Fe^{3+} ions [11]. Fig. 8b shows the angular dependence of the critical field in the bc plane measured at a temperature of T = 4.2 K. In

addition, the data of the magnetic measurements at $\varphi = 0°$ and $90°$ are presented (triangles). A certain discrepancy between the magnetic and microwave measurement data for the c axis is most likely caused by a slight deviation of the sample rotation plane from the rhombic bc plane.

Since the size of Mn-doped single crystals was insufficient, we could only measure the magnetodielectric properties at the electric field orientation $E||c$, while the magnetic field was applied along the three rhombic axes. The field dependences of the relative change in the capacitance of a capacitor with the Mn-doped single crystal measured at T = 4.3 K and different orientations of the magnetic field are shown in Fig. 9a. Fig. 9b shows these dependences for the undoped $Pb_2Fe_2Ge_2O_9$ crystal from [6]. For convenience of the comparison, the plots were built in the same scale along the vertical axis. The capacitance change $\Delta C_d/C_0$ was normalized to its value at $H = 0$. At the $E||c$ and $H||a$ orientations, the magnetodielectric response in the Mn-doped crystal is almost independent of the magnetic field. In the magnetic field applied along the b axis, the response depends on the field very weakly; however, no anomalies were found in the region of the orientational transition. Only in the magnetic field $H||c$, we observed a sharp jump in the magnetodielectric response around the orientational transition. The value of this jump is about 0.9%, which is approximately 3 times greater than the maximum jump in the response during the spin-flop transition in the undoped crystal [6]. In addition, we should note the hysteresis of the magnetodielectric response, which corresponds to the hysteresis of the orientational transition at the forward and inverse magnetic field scanning.

4. Discussion

In [5], we attempted to explore the magnetic structure of pure $Pb_2Fe_2Ge_2O_9$ by elastic neutron scattering. The neutron diffraction data clearly demonstrated that the magnetic structure of the crystal is complex antiferromagnetic, but the detailed magnetic structure was not established. However, the magnetic study allowed us to unambiguously state that the equilibrium direction of the antiferromagnetic vector in this crystal coincides with the c axis and the spin-flop transition was observed in the same direction. In the doped crystal, the orientational transitions occur both in the b and c orthorhombic direction. In addition, due to doping, the spontaneous weak ferromagnetic moment in the a axis direction vanished. The temperature dependences of the magnetic susceptibility for the doped and pure crystals also differ, pointing out a significant change in the magnetic structure upon doping.

Such significant changes can be explained in several ways. At first sight, it seems that doping of the crystal with the highly anisotropic Mn^{3+} ion caused such a change in the magnetic anisotropy of the crystal that the equilibrium direction of its easy anisotropy axis deviated from the c axis. This can happen if the local easy anisotropy axes for the Mn^{3+} ion are close to the b axis. Due to the competition of anisotropic contributions in the crystal, an inclined magnetic structure forms, in which the antiferromagnetic vector lies in the rhombic bc plane and, when the field is oriented along both the b and c axis, projections of the spin-flop transition to these directions are observed. Moreover, the critical field for the c direction is significantly weaker than for the b axis, which suggests that the easy magnetization direction lies in the bc plane closer to the c axis. The angular dependence of the critical field in this plane does not contradict this fact; the minimum critical field in this dependence corresponds to the field orientation at an angle of $\varphi \approx 15–20°$ to the c axis.

Meanwhile, some experimental facts are inconsistent with this explanation. First, in this case, the angular dependence of the critical field would have to be described by the simple relation $H_c(\varphi) = H_c^{min}/cos(\varphi - \varphi_0)$. This dependence is shown in Fig. 8b (solid line) and its agreement with the experimental data is unsatisfactory.

Another issue that contradicts this explanation is the fundamental difference between the behaviors of the field dependences for the b and c
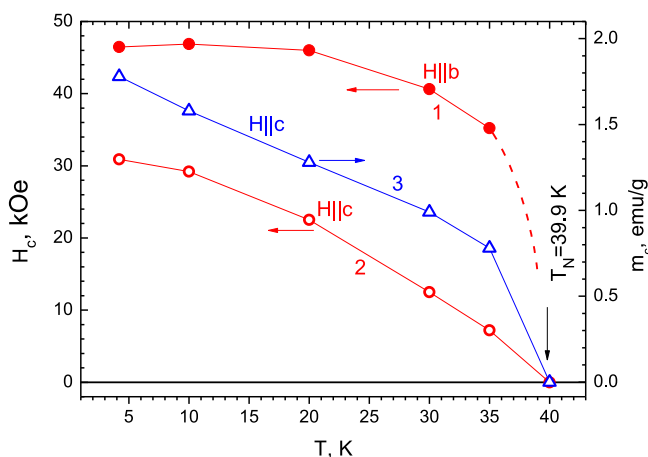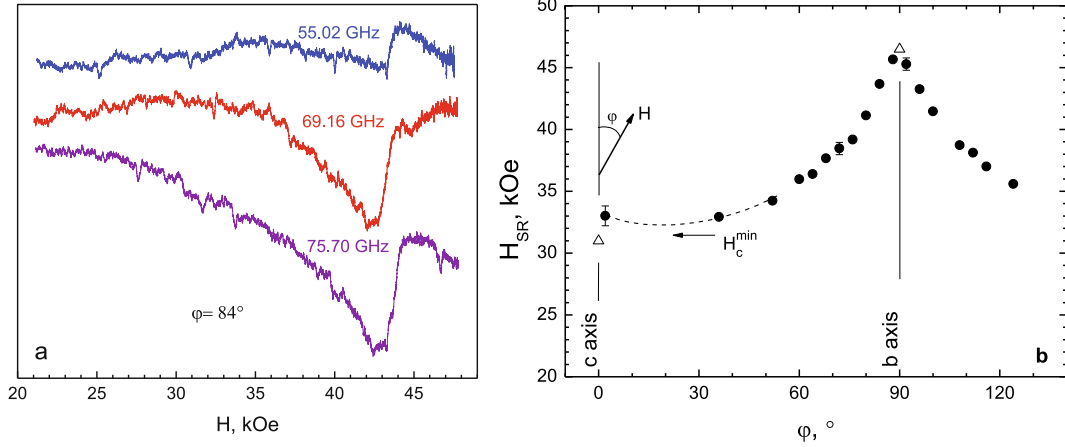

Fig. 7. Temperature dependences of the critical transition fields at $H||b$ (curve 1) and $H||c$ (curve 2) and weak ferromagnetic moment m_c (curve 3).

Fig. 8. (a) Fragments of the spectra showing the nonresonance microwave response corresponding to the spin reorientation. (b) Angular dependence of the critical field H_{SR} in the **bc** plane (circles) and magnetic measurement data (triangles). T = 4.2 K.
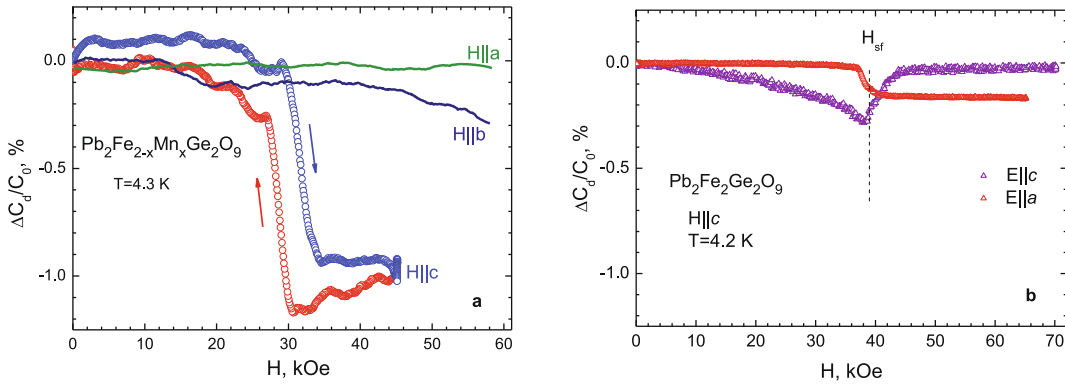
Fig. 9. Field dependences of the magnetodielectric response in (a) $Pb_{2-x}Mn_xFe_2Ge_2O_9$ at $E||c$ and (b) $Pb_2Fe_2Ge_2O_9$ at $E||a$ and $E||c$.

axes. Under magnetization along the **b** axis, the above-mentioned ratio between the magnetic susceptibilities above and below the transition is observed. At the same time, the initial magnetic susceptibility for the **c** axis is not only no lower than the susceptibility above the transition, but even slightly exceeds it. The temperature dependences of the transition critical fields for the **b** and **c** axes are also different.

All these facts allow us to assume that the magnetization jumps detected in the field dependences for the **b** and **c** axes correspond to different orientational transitions. Let us consider the field dependence of the magnetization at $H||b$ (Figs. 4 and 5). The shape of this dependence is typical of the spin-flop transition at which the loss of the magnetic anisotropy energy in the spin-flop state is covered by the gain in the Zeeman energy due to the difference between the magnetic susceptibilities ($\chi_\perp - \chi_{||}$). This gives us grounds to believe that, in the Mn-doped crystal, the **b** axis becomes the easy magnetization axis, in contrast to the pure crystal, in which the antiferromagnetic vector in the ground state is directed along the **c** axis [5,6]. The nonmonotonic character of the temperature dependence of the critical field H_{SR}^b (see Fig. 7) is typical of such a mechanism of the orientational transition.

Let us compare the magnetic structures of the pure and Mn-doped crystals using the thermodynamic potential for a two-sublattice rhombic crystal and a centrosymmetric exchange structure with the second-order axis along the rhombic **b** axis, relative to which the antiferromagnetic structure is even [17–19]

$$F = Am^2 + a_1 m_x^2 + a_2 m_z^2 + b_1 l_x^2 + b_2 l_z^2 + d_1 m_x l_z + d_2 m_z l_x - hm. \quad (1)$$

The expansion was made over the components of the ferromagnetic vector $m = (M_1 + M_2)/2M_0$ and the antiferromagnetic vector $l =$

$(M_1 - M_2)/2M_0$; A is the exchange constant; a_1, a_2, b_1, and b_2 are the magnetic anisotropy constants; d_1 and d_2 are the constants at the invariants responsible for weak ferromagnetism; and $h = H \cdot 2 M_0$.

According to the analysis made in [17], if the antiferromagnetic vector in the pure crystal in the ground state is directed along the **z** axis (the **c** axis), then the existence of weak ferromagnetism along the **a** axis due to the invariant $m_x l_z$ leads to the field dependence of the magnetization in this direction [17]:

$$m_x = \frac{d_1 + h_x}{A + a_1 - b_2} \quad (2)$$

with the weak ferromagnetic moment $M_{da} = m_a \cdot 2M_0 \approx \frac{H_{da}}{H_E} M_0$.

Under magnetization along the rhombic **c** axis in the spin-flop state, the vector l is parallel to the **a** axis and the weak ferromagnetic moment m_c in the **c** axis direction is caused by the invariant $m_z l_x$. This configuration leads to the field dependence of the magnetization for this state [17]:

$$m_z = \frac{d_2 + h_z}{A + a_2 - b_1}, \quad (3)$$

with the weak ferromagnetic moment $M_{dc} = m_c \cdot 2M_0 \approx \frac{H_{dc}}{H_E} M_0$

Let us now pass to the Mn-doped crystal. In this crystal, the antiferromagnetic vector in the ground state is directed along the **b** axis. Such a change in the magnetoanisotropic properties follows from doping with the highly anisotropic Mn^{3+} ion. The magnetic phase diagram of this crystal upon magnetization along the **b** axis is illustrated in Fig. 8a.

According to the form of thermodynamic potential (1), which does not include the mixed invariants with l_y, the spontaneous weak ferromagnetism is absent in this case (see state 1 in Fig. 10a). The absence of the spontaneous (i.e., for the magnetic field H → 0) weak ferromagnetism in this state is confirmed by the initial portions of the field dependences of the magnetization for all the rhombic axes (Fig. 4). Under magnetization along the b axis, a spin-flop transition is observed, which is induced by the difference between the magnetic susceptibilities above and below the transition. The absence of the $m_y l_i$ invariants in the thermodynamic potential prevents the occurrence of weak ferromagnetism along the b axis in the spin-flop state. However, in this state, weak ferromagnetism can arise in the transverse a or c direction, depending on orientation of the antiferromagnetic vector along the c or a axis in the spin-flop state (states 2 or 3 in Fig. 10a). Since, for this crystal, the anisotropy constants required for comparing the energies of these states are unknown, one of them can be chosen when measuring the field dependences of the transverse magnetization in the a and c axes directions for H||b.

In this crystal, the most interesting case is magnetization along the c axis, which can be explained as follows. At this magnetization, when the magnetic field is perpendicular to the antiferromagnetic vector, the initial magnetization portion is determined by the magnetic susceptibility $\chi_\perp$. When a certain critical field is reached, the antiferromagnetic vector reorients stepwise to the rhombic a axis direction, which is accompanied by a magnetization jump induced by the weak ferromagnetic moment occurring in the c axis direction (state 4 in Fig. 10b, coinsiding with state 3). As in the pure crystal, this moment is induced by the invariant $m_z l_x$ and the field dependence of the magnetization above the critical field is described by Eq. (3). Obviously, in this state, the field dependence is also determined by the perpendicular magnetic susceptibility $\chi_\perp$. The similar transitions were observed, for example, in orthorhombic antiferromagnets with weak ferromagnetism YFeO$_3$ and YCrO$_3$ [20,21].

Thus, in the Mn-doped crystal, the spin reorientation in the c axis direction is not related to the difference between the perpendicular and parallel susceptibilities, but originates from the occurrence of a weak ferromagnetic moment in the field-induced state. The different nature of the orientational transitions under magnetization along the b and c axes leads to different temperature dependences of the critical field.

For the pure Pb$_2$Fe$_2$Ge$_2$O$_9$ crystal, the ground state is described by configuration 2 in Fig. 10a; configuration 3 corresponds to the spin-flop state upon magnetization along the c axis.

It is noteworthy that the weak ferromagnetic moments M_{dc} for the pure crystal and the crystal doped with Mn^{3+} ions are similar. It is well-known [17–19] that weak ferromagnetism in these antiferromagnets is caused by the two mechanisms: single-ion and Dzyaloshinskii–Moriya. Obviously, doping with the highly anisotropic Mn^{3+} ions significantly affects the single-ion contribution. The estimates obtained for pure Pb$_2$Fe$_2$Ge$_2$O$_9$ [6] suggest that the contribution of the antisymmetric

Dzyaloshinskii–Moriya interaction is dominant. The same ratio between the contributions of the single-ion and antisymmetric interactions to weak ferromagnetism was found in [21] for the YFeO$_3$ and YCrO$_3$ compounds, in which the ratios $|H_{si}/H_D|$ are no higher than 0.02 and 0.05, respectively. At such ratios between the single-ion and antisymmetric contributions, the similarity of the weak ferromagnetic moments M_{dc} for the pure and doped crystals is quite natural.

The proposed magnetic phase diagrams allow us to make an assumption about the nature of jumps in the magnetodielectric response during the spin-reorientation transitions in the pure and Mn-doped Pb$_2$Fe$_2$Ge$_2$O$_9$ crystals. According to the magnetic phase diagram of the pure crystal in the magnetic field H||c, in the ground state before the spin-flop transition the weak ferromagnetic moment M_{da} is directed along the rhombic a axis and, during the transition, it reorients stepwise to the c axis. It is reasonable to attribute the jump in the magnetodielectric response during the spin-flop transition to the change in the magnetization in the direction of the applied electric field E, i.e., perpendicular to the capacitor plates. In other words, in pure Pb$_2$Fe$_2$Ge$_2$O$_9$, the jump of the magnetodielectric response in the geometry E||c, H||c (Fig. 9b) is caused by the occurrence of the moment M_{dc}||E_c at the spin-flop transition and the response jump in the geometry E||a, H||c is explained by vanishing of the moment M_{da}||E_a during the same transition. The jump at E||a twice as small as the jump at E||c can be attributed to the fact that, in the spin-flop state, the moment M_{dc} is almost twice as high as the moment M_{da}. At the other combinations of the mutual orientation of the magnetic and electric fields in pure Pb$_2$Fe$_2$Ge$_2$O$_9$, no sharp magnetization changes occur in the direction perpendicular to the capacitor plates, which explains the very weak field dependence of the magnetodielectric response for these directions.

Let us consider the data of magnetodielectric measurements on the Mn-doped crystal. According to the magnetic phase diagrams proposed for this crystal (Fig. 10), under magnetization along the c axis in the initial state, the antiferromagnetic vector l is directed along the b axis and m = 0. In the spin-flop state, the vector l reorients to the a axis; during this transition, in the c axis direction, the weak ferromagnetic moment M_{dc} arises stepwise. Therefore, in the geometry E||c, H||c, during the transition, a magnetodielectric response anomaly is observed, which is related to the magnetization jump in the direction perpendicular to the capacitor plates. In the magnetic field H||a, orientational transitions do not occur and we have m = 0; therefore, the field dependence of the magnetodielectric response is almost absent and no anomalies are observed. At the H||b orientation, the orientational transition to one of two possible states 2 or 3 with the weak ferromagnetic vector m directed along the a or c axes occurs. The absence of anomaly in the magnetodielectric response in this case suggests that, most likely, in the state after the orientational transition, the configuration with l||c and m||a is implemented, which corresponds to state 2 in Fig. 10a. Then, the magnetization jump during the transition occurs in

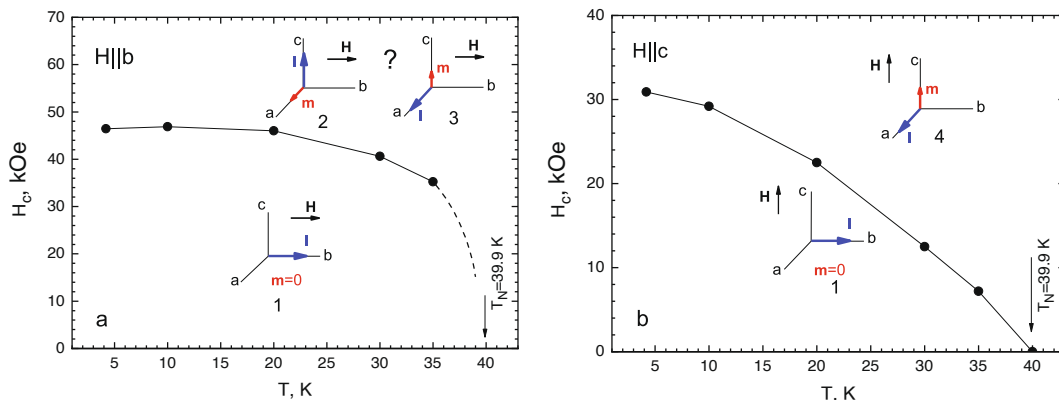**Fig. 10.** Magnetic phase diagrams of the Pb$_2$Fe$_{1.57}$Mn$_{0.43}$Ge$_2$O$_9$ crystal at the magnetic field orientations (a) H||b and (b) H||c.

the capacitor plane, rather than perpendicular to it, which explains the absence of anomaly in the response during such a transition.

An indirect confirmation in favor of configuration 2 for the spin-flop state at $H||b$ can also be the occurrence of a parasitic weak ferromagnetic moment upon magnetization in this direction. A feature of these single crystals is that they crystallize in the form of a parallelepiped elongated along the c axis with side faces parallel to the $(1\,1\,0)$ diagonal planes. With such a single crystal habit, the inaccuracy of sample positioning just in the ab plane is the most probable. In the spin-flop state, the inaccuracy of setting the sample in the b axis direction leads to admixture of the weak ferromagnetic moment arising in configuration 2 in the a axis direction.

The possible origin of the anomaly of the magnetodielectric response during the orientational transition in the undoped crystal was discussed in [6]. It was shown there that the observed jumps in the response $\Delta C/C \sim 3 \cdot 10^{-3}$ cannot be explained by the effect of magnetostriction, since it would require too large magnetostriction constants. In the Mn-doped crystal, the response jump increased to about $\Delta C/C \sim 1 \cdot 10^{-2}$, which so much the more allows us to exclude the magnetostriction mechanism. Another possible explanation of the effect can be based on the permittivity variation at the spin-reorientation transition due to the magnon–phonon coupling [6]. The partial substitution of the highly anisotropic Mn^{3+} for iron ions apparently led to the significant strengthening of the magnon–phonon coupling, which intensified the response at the orientational transition by a factor of 3 as compared with the undoped crystal.

In addition, we synthesized the $Pb_2Fe_{2-x}Mn_xGe_2O_9$ ($x = 0.2$) single crystals (according to the charge composition) and preliminary investigated their magnetic properties. The data obtained suggest that the magnetic structure of these crystals is intermediate between the structures of the compositions with $x = 0$ and 0.43. The antiferromagnetic vector in the crystal most likely holds a position in the rhombic bc plane that is intermediate between $l||c$ in the pure crystal and $l||b$ in the doped crystal with $x = 0.43$. After thorough investigations of the magnetic and thermodynamic properties of the crystal, the results will be reported elsewhere.

5. Conclusions

The $Pb_2Fe_{2-x}Mn_xGe_2O_9$ ($x = 0.43$) orthorhombic antiferromagnet single crystals were synthesized by a modified spontaneous crystallization pseudo-flux technique with partial substitution of the highly anisotropic Mn^{3+} ion for iron ions.

The measured temperature and field dependences of the magnetization are indicative of a drastic change in the magnetic structure as compared with that of the undoped crystal. In the magnetic field oriented along the orthorhombic b and c axes, magnetization jumps were detected, indicating the occurrence of orientational transitions under magnetizing in these directions. In both cases, the significant magnetization hysteresis observed during the transitions pointed out that the transitions were first-order. The weak ferromagnetism characteristic of the pure crystal in the rhombic a axis direction was not found.

The field dependences of the magnetization of the pure and Mn-doped crystals were analyzed based on the thermodynamic potential written with allowance for the crystal symmetry. It was shown that, in the Mn-doped crystal, the antiferromagnetic vector in the ground state is parallel to the rhombic b axis; in this state, there is no weak ferromagnetism. Under magnetization in this direction, we observed a conventional spin-flop transition induced by the difference between the perpendicular and parallel magnetic susceptibilities. When the crystal is magnetized along the rhombic c axis, then, after reaching the critical field, the antiferromagnetic vector rotates stepwise from the b to a axis and a weak ferromagnetic moment arises in the c axis direction, leading to the magnetization jump. Based on the field dependences of the magnetization measured at different temperatures along the rhombic b and c axes, the magnetic phase diagrams of the Mn-doped crystal in the

magnetic fields $H||b$ и $H||c$ were built.

In the Mn-substituted crystal at $E||c$ and $H||c$, a jump in the magnetodielectric response induced by the orientation phase transition was found. This jump was 3 times as high as the analogous jumps in the undoped crystal. At the magnetic field orientation $H||b$, no anomalies in the magnetodielectric properties around the spin-flop transition were observed and, at $H||a$, the field dependence of the response was also almost absent. The anomalous behavior of the magnetodielectric properties near the orientational transitions in the pure and Mn-doped crystals were analyzed using the magnetic phase diagrams for both crystals. It was assumed that, in both crystals, the anomalies in the magnetodielectric properties induced by the orientation transitions can be related to the fact that, during the transition, a weak ferromagnetic moment arises or vanishes in the direction parallel to the electric field in the crystal.

Declaration of Competing Interest

The authors declare that they have no known competing financial interests or personal relationships that could have appeared to influence the work reported in this paper.

References

[1] D.I. Khomskii, JMMM 306 (2006) 1.
[2] S. Ivanov, R. Tellgren, H. Rundlof, N. Thomas, S. Ananta, J. Phys.: Condens. Matter 12 (2000) 2393.
[3] I.P. Raevski, S.P. Kubrin, S.I. Raevskaya, V.V. Titov, D.A. Sarychev, M. A. Malitskaya, I.N. Zakharchenko, S.A. Prosandeev, Phys. Rev. B 80 (2009), 024108.
[4] J. Barbier, D. Levy, Acta Cryst. C54 (1988) 2.
[5] G.A. Petrakovskii, M.A. Popov, A.D. Balaev, K.A. Sablina, O.A. Bayukov, D. A. Velikanov, A.M. Vorotynov, A.F. Bovina, A.D. Vasil'ev, M. Boehm, Phys. Solid State 51 (2009) 1745.
[6] A.I. Pankrats, D.A. Balaev, S.E. Nikitin, A.L. Freydman, A.A. Krasikov, A.D. Balaev, S.I. Popkov, M.I. Kolkov, JMMM 479 (2019) 114.
[7] A.A. Demidov, I.A. Gudim, E.V. Eremin, JETP 115 (2012) 815.
[8] A.K. Zvezdin, A.M. Kadomtseva, Yu.F. Popov, G.P. Vorob'ev, A.P. Pyatakov, V. Yu Ivanov, A.M. Kuz'menko, A.A. Mukhin, L.N. Bezmaternykh, I.A. Gudim, JETP 109 (2009) 68.
[9] R.P. Chaudhury, F. Yen, B. Lorenz, Y.Y. Sun, L.N. Bezmaternykh, V.L. Temerov, C. W. Chu, Phys. Rev. B 80 (2009), 104424.
[10] A. Pankrats, K. Sablina, M. Eremin, A. Balaev, M. Kolkov, V. Tugarinov, A. Bovina, JMMM 414 (2016) 82.
[11] A. Pankrats, M. Kolkov, A. Balaev, A. Shabanov, A. Vasiliev, JMMM 497 (2020), 165997.
[12] G. Dörsam, A. Liebscher, B. Wunder, G. Franz, Am. Mineral. 93 (2008) 573.
[13] S.K. Barbar, B. Kumar, O. Prakash, et al., Ceramics International 46 (2020) 28716.
[14] J. Ito, C. Frondel, Am. Mineral. 53 (1968) 1276.
[15] A.D. Balaev, Yu.V. Boyarshinov, M.M. Karpenko, B.P. Khrustalev, Prib. Tekh. Eksp. 3 (1985) 167.
[16] V.I. Tugarinov, I.Ya. Makievskii, A.I. Pankrats, Instrum. Exp. Tech. 47 (2004) 472.
[17] E.A. Turov, Physical properties of magnetically ordered crystals, Academic, New York, 1965.

[18] E.A. Turov A.V. Kolchanov V.V. Men'shenin, I.F. Mirsaev, V.V. Nikolaev, Symmetry and physical properties of antiferromagnets 2001 Fizmatlit, Moscow [in Russian].

[19] S.N. Martynov, JETP Lett. 108 (2018) 196.
[20] V.M. Judin, A.B. Sherman, I.E. Mylnikova, Phys. Lett. 22 (1966) 554.
[21] J.S. Jacobs, H.F. Burne, L.M. Levinson, J. Appl. Phys. 42 (1971) 1631.